Journal of Optoelectronic and Biomedical Materials Vol. 17, No. 4, October-December 2025, p. 237-250

# Impact of dilution and time on the antibacterial activity and potential for treating colon cancer of environmentally prepared nickel oxide nanoparticles from rosemary extract

S. M. Shtait, A. N. Abd *, N. J. Ghdeeb
*Physics Department, College of Science, Mustansiriyah University, Baghdad, Iraq*

Recent research has concentrated on the enlargement of new biomedical agents. Consequently, the biosynthesis of nanoparticles has garnered important attention in recent years as a result of the increased development of new pathogens and microbial resistance against antibiotic therapy. The green synthesis approach is used in this work to generate "nickel oxide nanoparticles" NiO NPs utilizing nickel nitrate as a starting material and plant extracts from rosemary as a reducing agent and coating. Multiple characterization techniques have been used to classify the composite nanoparticles, including XRD, which confirmed the crystallinity of NiO NPs at face centered cubic phase at average size of crystalline is 13.59 nm. Fourier transform infrared spectra confirmed the NiO formation with high purity phase, which was found at the range 827 ($cm^{-1}$). The FE-SEM shows that the nanoparticle size is 17.69 nm, with spherical and semi-spherical forms of the Nano clusters, which is in good agreement with the XRD data. And according to AFM, the average size of particle of NPs is 57 nm. NiO NPs have an optical bandage of 3.8 and 4.5 eV, and notable emission peaks were seen in the visible and ultraviolet regions. Agar well diffusion was used to test the antimicrobial behavior of green synthesized nanoparticles against four distinct bacterial species: S. epidermidisa, S. aurous, K. pneumonia, E. coli, and C. albino's fungi. The results showed significant antimicrobial activity over time and at varying concentrations, and an MTT assay was used to determine the anticancer activity against human colon cancer cells (CL-40).Even at very low concentrations, NiO nanoparticles showed significant anti-cancer effects against human colon cancer cells CL-40 ($IC_{50}$: 69.20µg/mL). These findings imply that the synergistic effect of the green synthesized NiO nanoparticles physical characteristics and adsorbed phytomolecules on their surface may be responsible for their increased biological activities. "These results raise the possibility that NiO has new biological uses, such as as an antibacterial and anticancer agent".

(Received August 5, 2025; Accepted October 13, 2025)

*Keywords:* Green synthesis, Nickel oxide nanoparticles, Antimicrobial activity, Colon cancer

## 1. Introduction

Nanotechnology has at least one dimension, ranging less than 100 nm; it is possible to engineer materials by varying their size. As a result, their properties can be effortlessly changed by altering their size at the nanometer scale. Engineered transition "metal oxide nanoparticles" (M-O NPs) show unique chemical, physical, and biological properties that differ from those of their bulk counterparts, NPs. Because of these unique properties, nanoparticles are used in a variety of fields .They are also effective drug haulers for both "in vitro" and "in vivo," and they have an extensive range of applications, such as smart windows, photo catalysis, and anti-microbial activity. As a result, they have drawn a lot of attention. [1,2]

The synthesis of magnetic nanoparticles (NPs) of Fe, Co, and Ni has gained attention in recent years because of their exceptional magnetic qualities and possible applications in a variety of domains, such as sensors, memory storage devices, and catalysis. Magnetically regulated medication delivery, magnetic resonance imaging, and the treatment of cancer cells by

* Corresponding author: ahmed_naji_abd@uomustansiriyah.edu.iq
https://doi.org/10.15251/JOBM.2025.174.237

hyperthermia are among their applications in medicine [3]. NiO NPs with a wide band gap of 3.6 to 4.0 eV and a cubic lattice structure have potential because they are p-type semiconductors. They are important because of their unique magnetic, high chemical stability, super capacitance, electron transfer, and electro catalytic properties in energy technology, biomedicine, and photo catalytic, anti-inflammatory, and antimicrobial activities, which have attracted the scientific community [1]. Compared to micro and macro sized NiO particles, nanostructured NiO also has better qualities such as volume effect, surface effect, and quantum size effect [2]. NiO NPs were produced using a variety of methods, including chemical precipitation, sol-gel combustion, and solid state "chemical decomposition, solve thermal process, and reverse micro-emulsion approach". These techniques, however, need specialized equipment, high temperatures, and intricate procedures. Although they may yield well-defined pure NPs, they are not environmentally friendly and may even be harmful. They also have limited productivity, low antioxidant potential, and low antibacterial activity. Usually, the production of free radicals causes oxidative stress, which in turn causes nontoxicity. In the mineralization of microorganisms, the reactive oxidative species (OH and $O^{-2}$) are thought to be more prevalent and highly reactive than hydrogen peroxide ($H_2O_2$) and per hydroxyl radicals (HOO·) [2, 3].

Therefore, there is a lot of interest in creating environmentally benign processes that use bio nanotechnology, which creates NPs by applying biological systems including fungi, bacteria, plants, yeast, and naturally befalling fine molecules like proteins and vitamins. Plant extracts are primarily used in the production of nanomaterials because they are effective capping and reducing agents that can be used in place of chemical and photochemical reduction techniques. Additionally, because the porous portions of the plants serve as a bio template, a regulated morphology can be achieved in the reduction the ions of metal [2]. In order to create application-oriented NPs that give researchers the freedom to create NPs with the desired features, it is crucial to choose an appropriate synthesis approach [4]. In order to create NPs with the intended functions, physical and chemical methods are combined with biological principles by microbial enzymes or plant phytochemicals [3].Compared to chemically synthesized nanoparticles, green systems-synthesized nanoparticles are easy, affordable, environmentally benign and non-toxic, making them an attractive research topic [2]. In this study, nickel nitrate and rosemary leaf extract are chosen for the manufacture of NiO NPs. In the preparation process, the plant extract's function is to lower the salt content and generate the appropriate nano-M-O [5]. The project's goal is to manufacture nickel oxide nanoparticles (NPs), investigate their characteristics, and demonstrate their efficacy against cancer, fungi, and some types of bacteria, both positive and negative, while using materials of high economic quality and no toxicity.

## 2. Experimental section

**Reagents:** The inorganic compound nickel (II) nitrate, "Ni $(NO_3)_2.6H_2O$", has a molecular mass of 182.7 g/mol. It was acquired from British drug house (BDH) Chemicals Ltd Pool, England, were employed as the nickel element's source. Rosemary leaves plant were purchased from markets in Baghdad, Iraq, which will using it extract as a reducing agent. The plant is cultivated all over the world. According to figure (1), it grows into an aromatic evergreen shrub with upright forms that may grow up to 1.2–1.8 meters (4–6 feet) tall. Its evergreen leaves are "2–4 cm long and 2–5 mm broad, with a green upper surface and a white underside".

### 2.1. Synthesis of materials

#### *2.1.1. Preparation of rosemary plant extract*

First of all, leafs of rosemary are washed well by water, dry, and then milling into fine particles using a hander grinder. After that we take 2g of milling leafs particles and dissolved in 50ml of deionized water (DI water) in a (150) flat bottom beaker, heated with a hotplate magnetic stirrer at 60C° for 25 minute, until obtain a clear brown solution and "this solution was filtered using filter paper to get rid of the impurities, figure(1)."

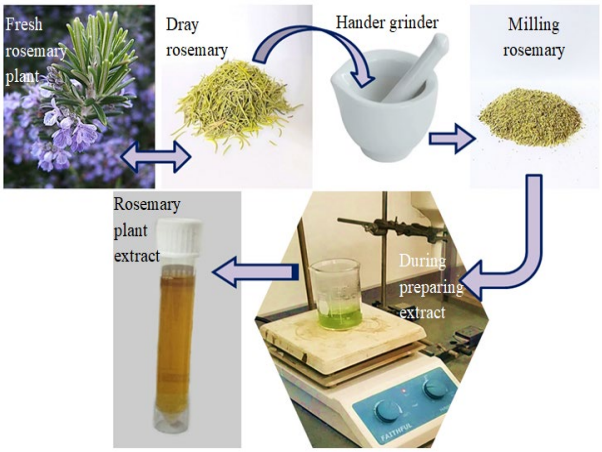


*Fig. 1. Steps involved preparing plant extract.*

***2.1.2. Preparation of NiO NPs:*** *According to relation (1) [6]:*

$$M = \frac{m}{M} \times \frac{1000}{v} \quad (1)$$

M: Molecular concentration (mole / L).
m.: The mass of a substance (g).
M: The molar mass of a substance (g / mole).
V: "The size of the instillation water in which the solubility has been dissolved (mL)" was taken a (0.91gm) of Ni $(NO_3)_2.6H_2O$ and added to beaker Contains 500 ml of deionized water after it has been on a hot plate magnetic stirrer for 25 minutes (until the nitrate is entirely dissolved), then 20ml of rosemary plant extract solution is gradually added to the mixture at the same temperature. As time passes, we notice that the colloidal hue color progressive changes from turquoise to dark olive, figure (2). That change in color considers an optical indicating that the final substance contains Nano scale nickel oxide (NiO NPs), that agrees with what finding at [7].

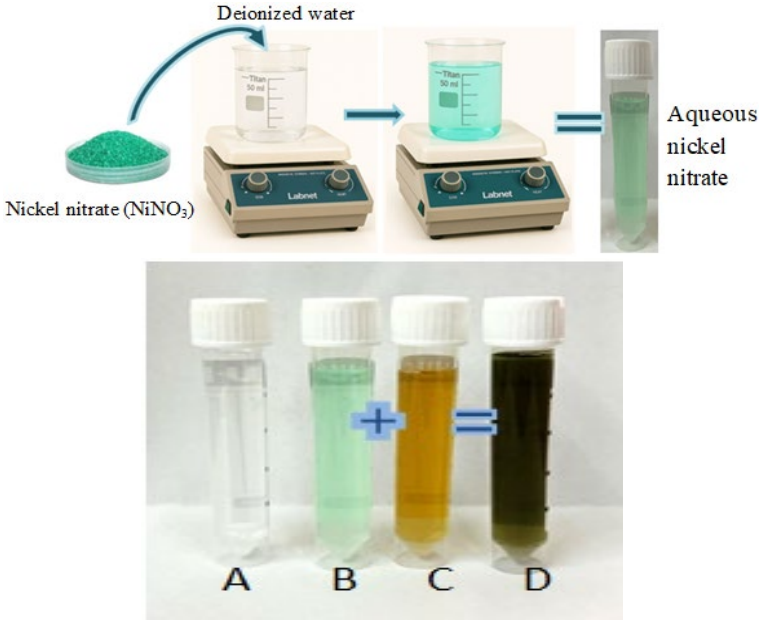


*Fig. 2. Stages of preparing NiO NPs colloidal and Experimental tubes containing A: distilled water; B: Aqueous nickel nitrate; C: Rosemary plant extract; D: resulting material containing nanoscale nickel oxide.*

The synthesized material was studied in its freshly prepared state without undergoing any calcination or annealing treatments (thermal modifications), this was done with the aim of studying in its synthesized form, and since that might have shifted its true antibacterial and anticancer effects.

***2.1.3. Preparation then film***

The colloidal solution made by green synthesis technique is deposited on the glass bases (2.5× 2.5 cm), for XRD, FE-SEM, AFM and FTIR analysis , by distilling the colloidal solution over those glass bases by drop casting technique using an electric heater set to (60) Cº, so the liquid evaporates after NPs is coated on the glass bases, We notice that at the beginning of the thin film formation process, its color is transparent, then it turns yellow, and gradually changes to dark gray as show in figure (3) ,and that is another optical indication of the success of the process in forming nickel oxide nanoparticle.

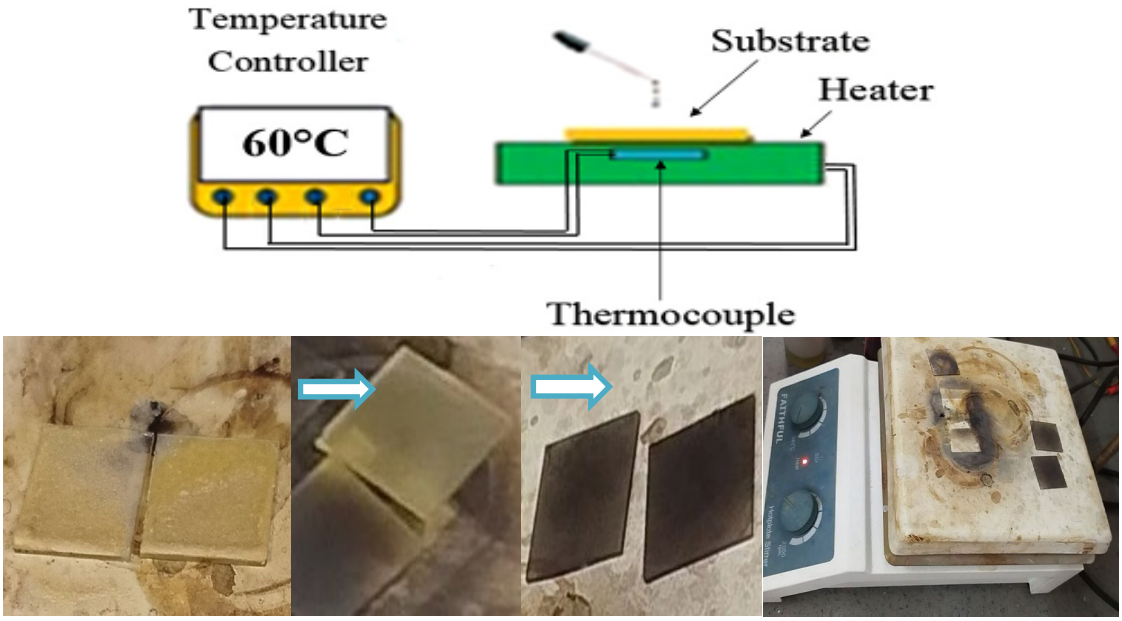


*Fig. 3. Drop casting technique to precipitate the solution of NiO NPs on a glass substrate.*

## 3. Result and discussion

### 3.1. Material Characterization

X-ray diffraction (XRD) and Fourier-transform infrared spectroscopy (FTIR) were employed to confirm the production of nickel oxide (NiO) NPs and how much its purity. The morphological features and particles size of the generated material were investigated by (FE-SEM) and (AFM), UV-visible spectroscopy was also used to assess the optical properties. After being characterized, the material was applied to assess its ability to inhibit against certain bacterial and fungal strains, and evaluate its cytotoxic impact on colon cancer cells.

### 3.2. Structural characterization

X-ray diffraction (XRD) and Fourier-transform infrared spectroscopy (FTIR) studies were both employed to determine the material that was generated and analyzing its crystal structure and chemical characteristics.

### *3.2.1. XRD diffraction*

This technique is based on the diffraction of X-rays, whose wavelength is equivalent to the distances between atoms in condensed matter. It is a very useful technique, which is used routinely to recognize the crystalline phases present in materials and analyze the materials' structural properties and various other structural parameters i.e. particle size, degree of crystallinity, orientation parameter and strains . In this investigation the XRD pattern with distinct peaks shows that the generated NiO NPs are pure and crystalline, figure (4). The vertical axis shows the X-ray intensity in arbitrary units (a.u.), while the horizontal axis shows the diffraction angle (Bragg angle), which varies between 40 and 80 degrees, According to the international standard [JCPDS 04-0835], the XRD peaks were found at 2θ angles of 37.04, 43.29, and 63.19, "which correspond to the (111), (200), and (220) planes, respectively". As a result, XRD analysis validates the creation of NiO NPs. The face-centered cubic (FCC) system is used to index all of the diffraction peaks [8,] which show the atomic distribution in the crystal lattice. It is confirmed that the synthesized NiONPs do not contain any impurities.

The appearance of background noise is indicative of the use of plant extract in the synthesis process, which is a commonly observed feature in green synthesis approaches (when don't do calcination or annealing treatments). With the use of the Debye-Scherer formula (equation (2)) [8], the crystallite size of the NiO NPs was determined, when the crystallites are in the nanoscale range the peaks become broader, according to the Debye–Scherrer equation D∝1/β:

$$D = \frac{K\lambda}{\beta cos\theta} \tag{2}$$

where, "$k$ equal to 0.9 (assuming to quasi-spherical morphology of NPs which found by FE-SEM analysis), λ equal to 1.5418 A ˚ (popularly known as Cu $K_\alpha$ radiation), β and θ are the X-ray wavelength, full width at half maximum (FWHM) of XRD peaks (can be calculated from the graph between intensity and 2θ), and angle of Bragg diffraction(will be known in the XRD instrument), respectively. The micro-strain (η) and the dislocation density (δ) were calculated by the following two equations [9]:

$$\delta = \frac{\beta cos\theta}{4} \tag{3}$$

$$\eta = \frac{1}{(D)^2} \tag{4}$$

Table 1 shows the structural parameters of NiO NPs Synthesis by Rosemary plant extract.

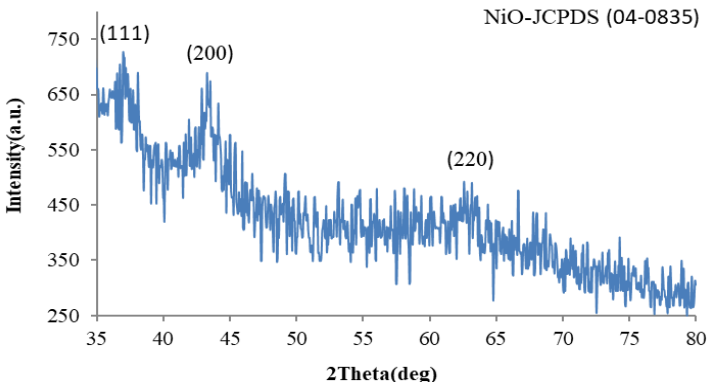


*Fig. 4. XRD pattern of NiO NPs Synthesis by Rosemary plant extract.*

*Table 1. Structural parameters of NiO NPs Synthesis by Rosemary plant extract.*

| 2 Theta (Deg) | FWHM (Deg) | D (nm) | $\eta x10^{-4}$ | $\delta x10^{14}$ (lines/$m^2$) |
|---|---|---|---|---|
| 37.04 | 0.8 | 12.40 | 27.93 | 65.00 |
| 43.29 | 0.8 | 13.61 | 25.44 | 53.92 |
| 63.19 | 1.2 | 14.76 | 23.46 | 45.87 |

The table above confirms the formation a very small crystalline size from particles of nickel oxide, where the average crystalline size is 13.59 (nm) which shows by the broad peaks in X-ray diffraction. And it clear that the micro-strain and the dislocation density decreases with increase the crystalline size, that mean the larger crystalline tend to stabilize.

### *3.2.2. FT-IR analysis*

The Fourier Transform Infrared characterization of the sample , as displayed in Figure (7), for the range of effective wavelengths just from 500 to 4000, we find the presence of multiple unique peaks, The successful creation of NiO is suggested by the first peak, which is located at 827 ($cm^{-1}$) it shows the special vibrations of the nickel oxide bond, Furthermore, this is consistent with [10,11], The peaks appeared at around 1402 (1/cm) it assigned to CH, Phenols or aromatic compounds are the cause of these peaks ,as in [12]. The C=O bond is included in the region 1640 ($cm^{-1}$) which is carboxyl compounds may be responsible for this peak, it consistent with [11,13,14]. Double bonds C=C are indicated by the bending vibration at 2402 ($cm^{-1}$) which are caused by the existence of an aromatic stretching vibration band as in [10, 11] .The OH vibrational overtone is identified by the peak in the spectra at rang 3282 to 3551 (1/cm), as in [11,15, 16].

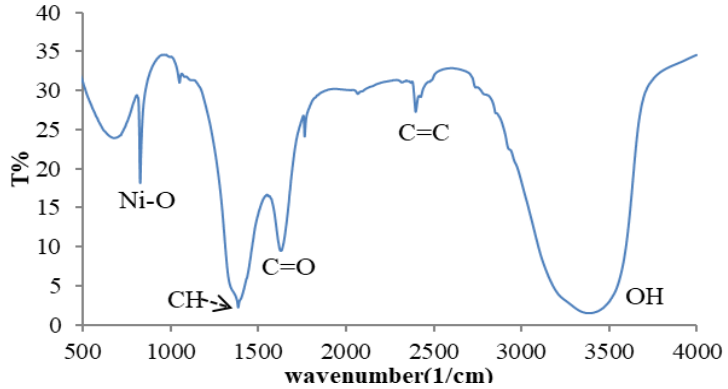


*Fig. 7. FT-IR spectrum for the transmittance of NiO NPS.*

We notice from the figure that the active bonds NiO appearance clarity, sharp and distinctive peak which found at the range 827 ($cm^{-1}$), this confirms the formation of high-purity nickel oxide nanoparticles. This supports the XRD result which confirmed that the synthesized NiONPs do not contain any impurities.

### 3.3. Morphology and compositional analysis

The surface morphology and topography of the NiO nanoparticles was explored using FE-SEM and AFM studies

### 3.3.1. FE-SEM studies

FE-SEM image for investigate a morphological characteristic of NiO NPs, the figure (5) show image with a magnification of 35kx in scale 1µm which gives a wider perspective of the produced thin film's surface, revealing any pores or structural gaps. The shape of obtained Nano-

particles become more clearly when magnified by 135kx with scale 200 (nm),which take a spherical or quasi-spherical shape and they are grouped together in cloud-like Collectives or Resemble the top of the trees with 17.69 (nm) dimensions. Agglomerated nanoparticles, as shown in FESEM pictures, are unavoidable during green synthesis since the phytochemical content of the bioextract is not controlled [17].

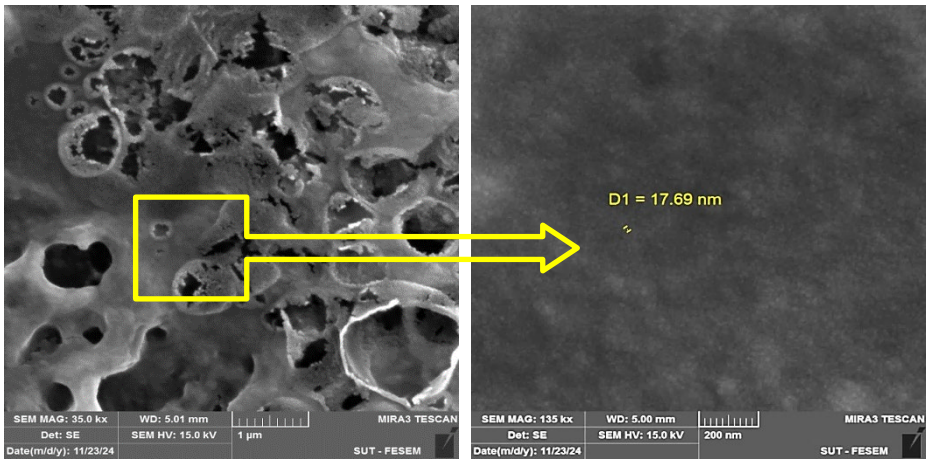


*Fig. 5. FE-SEM image of NiO NPs.*

Since the morphology of the NPs is not completely identical and is composed of numerous tiny, irregular, quasi-spherical NPs with diameters of (17.69) nm, we can confirm the different morphology of the particles from the FE-SEM images. The nanoparticle size determined from the XRD spectrum and the size determined from the SEM pictures were roughly in good agreement.

### *3.3.2. AFM studies*

Atomic force microscopy was used in this work to view and examine the surface's topographical features. The granularity accumulation distribution chart and 3D AFM images of NiO NPs, which were created by green synthesis and then deposited onto a glass substrate, are shown in figure (6). We observe that particles are arranged horizontally in different shapes aligned vertically as peaks upwards and distributed uniformly and homogeneously, resembling the gravel spread on the surface. We observe particles with dimensions ranging from 2 nm to 90 nm, with the highest concentration density at the particle size of (72 nm), according to the valued values of the root mean square (RMS) of the surface, roughness average, and average grain size, listed in Table (2) and from the Gaussian distribution.

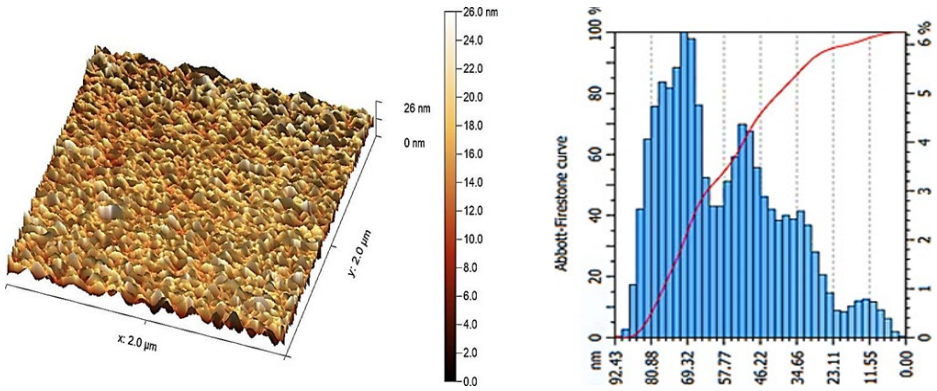


*Fig. 6. AFM images and histogram of NiO NPs.*

*Table 2. The average value, Root mean square and and roughness average of NiONPs.*

| Average value | RMS | Mean roughness |
|---|---|---|
| 57(nm) | 3.47 (nm) | 2.85 (nm) |

### 3.4. Optical properties

#### *3.4.1. UV-Vis analysis*

The absorption spectrum for NiO NPs is shown as a variable to the wavelength in the range of 200–1110 nm in figure (8). The wavelength of 222 nm is where we find the highest absorption, 0.81. It then decreases off quickly till it reaches 0.28 at a wavelength of 254 nm. Furthermore, we see that the quantum size effect causes notable differences in absorption spectra at wavelengths of 262 and 372, these peaks indicate the presence of NPs that correspond to Plasmon's, which is consistent with the notion of quantum confinement [9]. Then its value decreases to 0.02 nm over a wavelength range above 1077 nm. The band gap value of nickel oxide nanoparticles is determined by optical data using optical absorption (α) and photon energy (hv) using the Tauc plot [9]:

$$\alpha hv = \beta(hv - E_g)^n \tag{5}$$

where "(α) is the absorption coefficient which is proportional with the absorption, (h) is Planck's constant (J.s), (v)is the frequency of light ($s^{-1}$), Eg is the band gap energy,β is a transition constant and the exponent n depends on the type of transition (here n =1/2 for direct band gap transition).The energy band gap in NiO NPs was determined by extrapolating the tangent that intersects the x-axis at the point 3.8 and 4.5 (eV) which represents the energy gap, our results agree with[18] . The value of energy gap increases than its value at bulk and that is because of the quantum size effect (which indicated by XRD and FE-SEM), furthermore appearance multiple of energy gaps is explained by the increased concentration of charge carriers and the emergence of multiple allowed states for transition. [9].

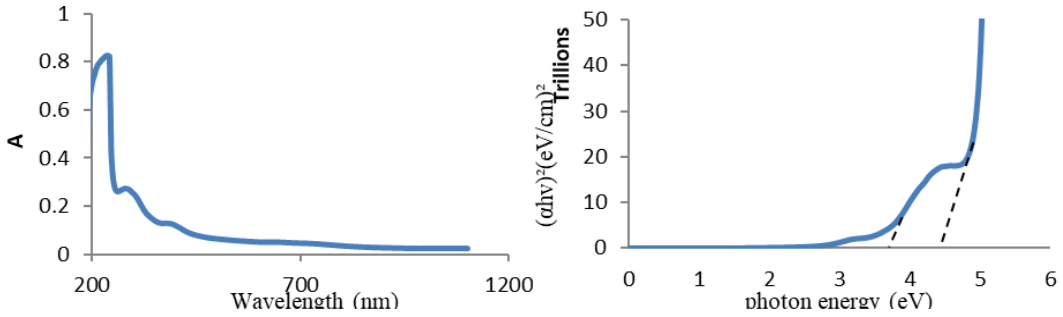


*Fig. 8. UV–Vis spectra: Optical absorbance and Energy gap of NiONPs colloidal.*

## 4. Cytotoxic effect

In the last decade, nanoparticles have broadly transpired as an antimicrobial agent, as it demonstrates specific targeting and minimal toxicity [11]. Thus, the biological activity of the synthesized material has been studied against two Gram positive and two Gram-negative bacterial strains, one fungal strain, as well as colon cancer cells. The antibacterial effects were performed in three stages at 37°C: once after 24 hours of synthesis, and once more after three months (90 days) following the date of the initial testing, the second stage was carried out to ascertain how time affected the manufactured material's efficacy (to look into their stability over time). After its prolonged bioactivity was confirmed, Different doses of the substance were tested for their inhibitory effects on microbial strains and tested agent colon cancer cells

**4.1. Antimicrobial activity**

**Microbial:** Technique name agar well diffusion was used in this study to assess the impact of synthesized NiO NPs on various bacteria and fungi, including Gram-positive bacteria like S. epidermidis and S. aureus and Gram-negative bacteria like K. pneumonia and E. coli. As well as pathogenic fungi like "Candida albicans"

**Inhibitory:** We note the biological effect (24 hours after production), or the so-called inhibition in the form of closed circles with a diameter as shown in Table (3), the synthesized nickel oxide exhibited inhibitory activity against all tested bacterial and fungal species, indicating its broad-spectrum antimicrobial efficacy. largest of inhibitions zone observed against fungi "C. albicans" , Afterward, the bacteria "K. pneumonia" then "S. epidermidis" and "E. coli" which it same diameter of inhibitions zone then for "S. aureus ", respectively as show in figure (9), suggesting a greater susceptibility of fungi compared to bacteria. After 3 months of preparing the materials, the test was repeated, and the results were shown also in Table (3). As seen in figure (10), we find that the inhibition zone's diameter generally decreases for all kinds of microbial. The inhibition zones for all bacterial species and fungi, dropped by an average of 1–6 mm, as can be seen when comparing the result at table (3), also re-evaluated the antimicrobial activity of NiO NPs by using different concentrations (25, 50, and 75 µg/mL) to determine the stability of NiONPs and determine how concentration effects on its stability and effectiveness. The results in table (4) show that ,inhibitory effect demonstrated a concentration-dependent, as proven by the increasing of inhibition zone with higher concentrations, as in figure (12) largest of inhibitions zone observed at 75 % ,50% then by 25% for bacteria "S. aureus "Afterward against fungi "C. albicans" , then against the bacteria "K. pneumonia" and "E. coli" " which have same diameter of inhibitions zone then for" S. epidermidisa", respectively.

**Mechanism of action (MOA):** The technology used, sample dosage, and treatment duration are the primary determinants of the activity of metallic nanoparticles as green synthesized nanostructures. The antibacterial action of NiO NPs is determined by their chemical composition, size, shape, and concentration. The antimicrobial activity of NiO NPs is mediated by changes to the cell membrane and blockage of transport channels. Ionization is produced when metallic ions the size of nanoparticles enter a cell; this can damage intracellular structures and ultimately result in cell death [2,11].When NPs reach the cell, they interfere with mitochondrial functions, destabilize the ribosome, damage proteins and enzymes, and live in the electron transport chain. Furthermore, by blocking cell division and the respiratory chain, these NPs actively disrupt DNA-like transcriptional mechanisms and result in cell death [19]. Additionally, because their cell walls are more permeable to Nano compounds, some Gram-positive bacteria might be more sensitive. Nano composites are less sensitive and have reduced permeability because gram-negative bacteria have more complex cell walls with an outer layer of lipopolysaccharides (LPS) [15].And the deficiency that occurred in the inhibition zone after three months is attributed to several reasons, including the possibility that NPs may combine over time, leading to aggregation or agglomeration, thereby forming larger particles, This reduces their ability to penetrate bacterial cell walls, Or due to the degradation of plant compounds such as phenols and flavonoids found in plant extracts, which reduces their enhancing effect on nickel oxide activity in inhibiting bacteria. It is noteworthy that the inhibition zone increases with the concentration of the substance, which may lead to a decrease in particle size and consequently an increase in the surface area to volume ratio, enhancing its ability to inhibit bacteria and fungi [19].

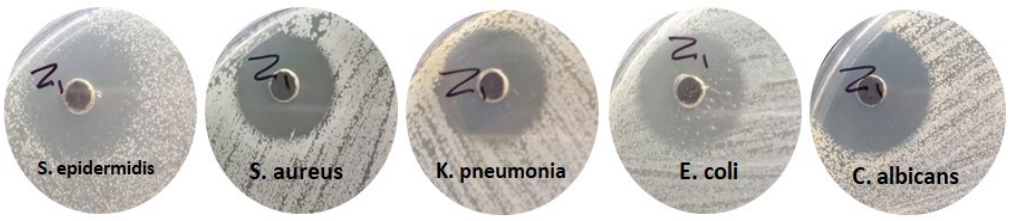


*Fig. 9. Antimicrobial activity of NiO NPs after 24 hours of preparation against.*

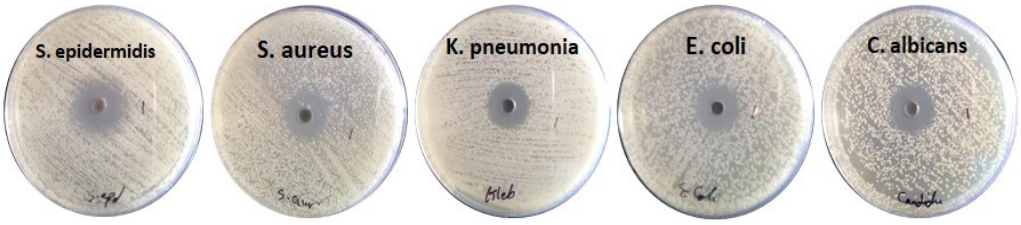


*Fig. 10. Antimicrobial activity of NiONPs After three months of preparation.*

*Table 3. Bio-synthesized NiO NPs by rosemary plant extract inhibitory zones (mm) against a subset of microorganisms of interest.*

| Test pathogens | Inhibition zone (mm) After 24 hours of preparation | Inhibition zone (mm) After three months of preparation |
|---|---|---|
| S. epidermidisa | 23 | 22 |
| S. aureus | 22 | 20 |
| K. pneumoniae | 25 | 21 |
| E. coli | 23 | 20 |
| C. albicans | 28 | 22 |

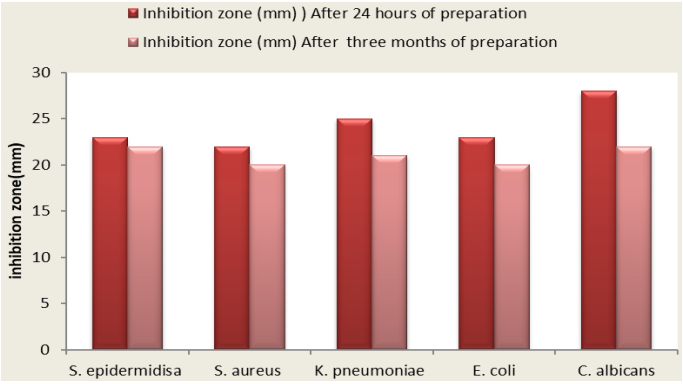


*Fig. 11. The inhibition for NiO NPs at different time.*

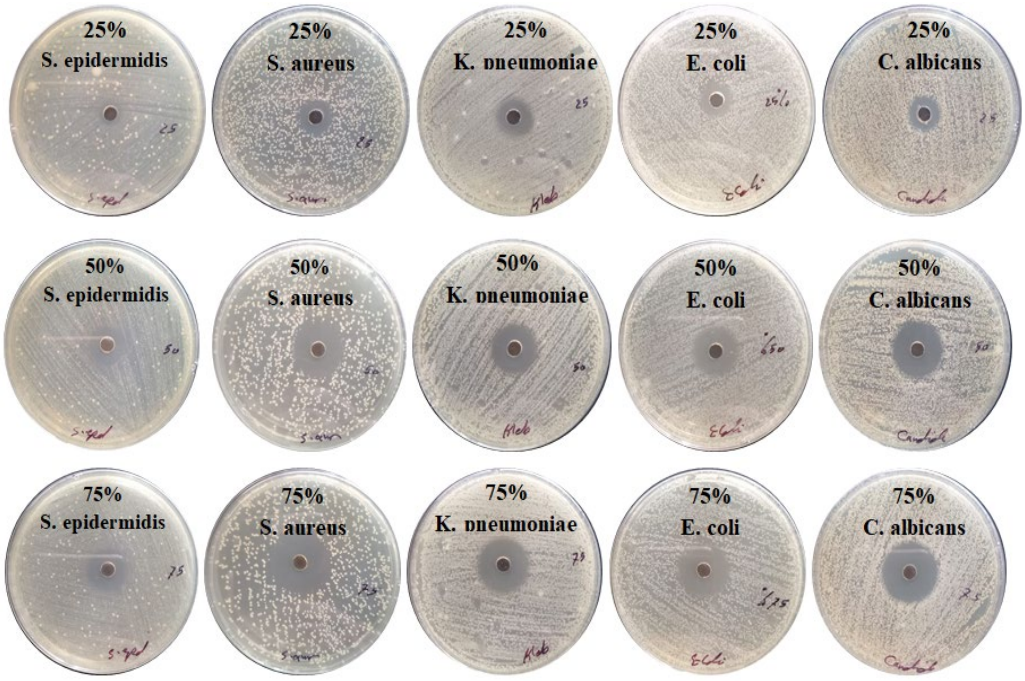


*Fig. 12. Antimicrobial activity of NiO NPs After three months of preparation at different concentration ( 25%, 50%, 75% M).*

*Table 4. Zone of inhibitions (mm) of biosynthesized NiO.*

| Test pathogens | Inhibition zone (mm) After three months of preparation at different concentration (25%, 50%, 75% M) | | |
|---|---|---|---|
| | **25%** | **50%** | 75% |
| S. epidermidisa | 11 | 17 | 19 |
| S. aureus | 17 | 24 | 27 |
| K. pneumoniae | 15 | 20 | 24 |
| E. coli | 13 | 20 | 24 |
| C. albicans | 16 | 24 | 25 |

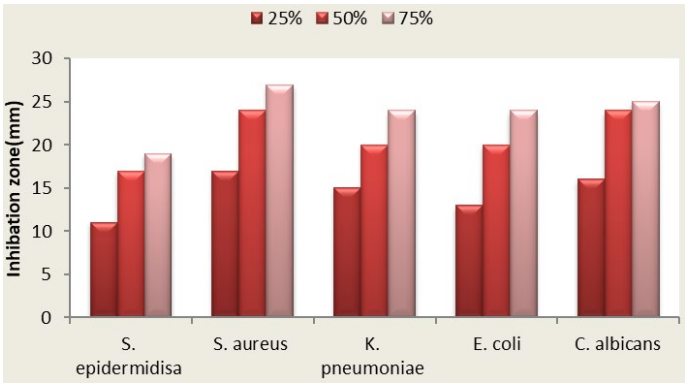


*Fig. 13. The inhibition zones (mm) for NiO NPs at different concentration (25%, 50%, 75% M).*

**4.2. Anticancer activity studies**

Today, research into nanoparticles for the diagnosis and treatment of cancer is increasing. In this study, we evaluated the cytotoxic effect of synthesized NiO-NPs by the usage rosemary plant extract on colon cancer CL-40 Cell line.

**Cell culture:** the cytotoxicity influences of NiO-NPs were examined on human (Homo sapiens) colon carcinoma (CL-40 Cell line) developed from a woman's right colon's primary colorectal cancer (TNM stage 3); the literature reported that the cells were highly differentiated. The line was sufficiently developed to form monolayers at 37°C in a humidified atmosphere with 5% $CO_2$. Throughout the assays, the cell line was grown in DMEM/HAM-F12 conditions without serum. Cells were cultivated in the medium at various intervals, as the tests showed. Aluminum foil was used to block the light from the cells. RA and DMSO were added one day after the cells were seeded to prevent any interactions with cell adherence to the culture dishes. Tumor cells were grown to about 90% confluence in each experiment, and then they were isolated into single-cell suspensions from tissue culture flasks using 0.05 percent EDTA in PBS for (3 min).

The MTT assay can reveal the number of dead cells following any treatment by counting the number of viable cells [20]. In 96-well plates, cells were cultured at concentrations ranging from 1 x 104 to 1 x 106 cells mL-1 until 200 mL of complete culture media was present in each well. After gently swirling and incubating the plates for 24 hours at 37 °C with 5% CO2, sterile Para film was used to cover them. Each well was supplemented with 200 µl of a materials NPs solution (25µg/mL), which was prepared by removing the medium and serially diluting it two times. We ran the concentration and control tests three times. After 24 hours of incubation at 37°C with 5% CO2, the plates were removed. Following the extract exposure, 10mL of MTT solution was applied to each well. The plates were then incubated for another 4 hours at 37°C with 5% CO2. After carefully removing the medium, each well was filled with 100 mL of DMSO solubilization solution and incubated for 5 minutes. At a wavelength of 575 nm, the absorbance was measured using an ELISA reader (Bio-rad, Germany). The untreated cells control (100% cell viability) was used to express the percentage of the cell viability. The IC50 was calculated using statistical analysis of the optical density values.

The calculated was doing according to the following formula [20]:

$$Viability(\%) = \frac{optical\ densty\ of\ sample}{optical\ density\ of\ control} \times 100\%$$

**Evaluation of cytotoxicity activity using NiO-NP:** The results of anticancer activity were in concordance with those of antimicrobial activity. The results demonstrated in figure (14) and Table (5) demonstrated that the viability of CL-40 cells was diminished in a concentration-dependent fashion, and that the survival rate of CL-40 cells was considerably decreased in a dosage-dependent manner ($P<0.0001$). At concentrations below 50 µg/mL, no differences can be seen, however between 50 and 1000 µg/mL, the apoptotic activity results are good. There was a cytotoxic impact on the cancer cells tested at all doses that were investigated.

**Apoptosis of cancer cells:** The antiapoptotic and pro-apoptotic proteins interact and determine cell fate in mitochondria, in which also the intrinsic pathway is primarily regulated [20]. The cytotoxicity action $IC_{50}$ was 69.20µg/mL, meaning that the nanoparticles destroyed about 50% of cells, which considered as the Half-maximal inhibitory concentration ($IC_{50}$).

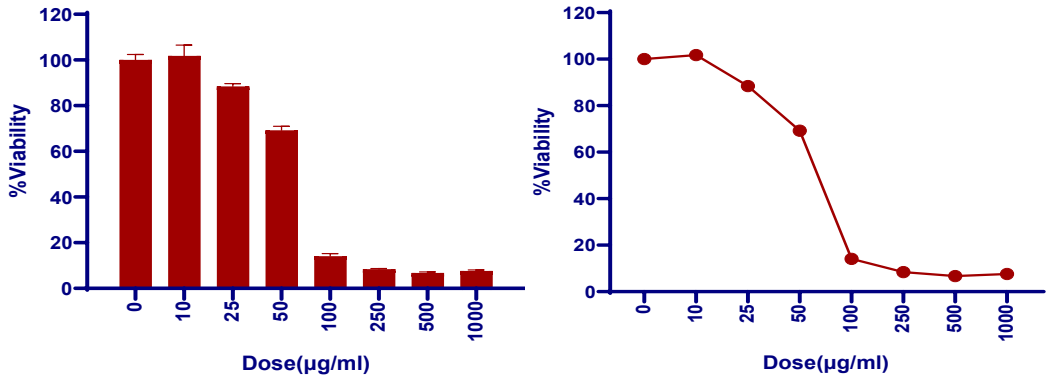


*Fig. 14. Anticancer activity of NiO NPs.*

*Table 5. Cell Viability (mean ± standard deviation (SD) of syntheses NiO NPs treatment on CL-40 cell line.*

| Dose(µg/ml) | Mean | SD | N |
|---|---|---|---|
| 0 | 100 | 2.365296263 | 3 |
| 10 | 101.7869657 | 4.677743833 | 3 |
| 25 | 88.43728104 | 1.231842736 | 3 |
| 50 | 69.20112126 | 1.766234501 | 3 |
| 100 | 14.08549405 | 1.136999351 | 3 |
| 250 | 8.409250178 | 0.315346882 | 3 |
| 500 | 6.727400143 | 0.458188396 | 3 |
| 1000 | 7.638402245 | 0.473992616 | 3 |

Evidence from previous in vitro models and epidemiological studies indicates that NiO NPs inhibit growth and induce apoptosis in a variety of cancer types. These characteristics of NiO nanoparticles may be related to antioxidant and other biological activities [21].and that also indicated by data showed at table above, even at low dose the inhibition was found, that show the potential of bioactivity of synthesis NiO NPs, that effect was increased with dose progressively, upon achieving almost total inhibition at increased dosages.

## 5. Conclusions

In the present study, NiO NPs were synthesized by eco-friendly method which it green synthesis using rosemary extract , NiONPs was identified and characterized using various techniques such as FTIR which proved formation of NiO NPs that they were in the range 827 (cm-1), XRD , FE-SEM, U.V-Visible and AFM, The XRD and FE-SEM studies that were done on them corroborated the shape and size of their crystals which equal to13.59 (nm) and 17.69 (nm) respectively who proves the Nano scale size of the formed particles.

Antimicrobial activity (Bacteria and fungi) results divulge that the NiO NPs have good potential to inhibit the growth of S.epidermidisa ,S. aureus , K.pneumoniae and E. coli bacteria and C. albicans fungi Over time and at different concentration , NiO NPs also demonstrated significant anti-cancer activity and good inhibition against human colon cancer cells (CL-40) until at very low concentration, According to findings at MTT assay results the $IC_{50}$ (69.20) µg/ml, Based on this study, it is possible to propose green produced NiO NPs as a potential biomedical agent substitute .

## References

[1] Haider, Ali, et al., Nanoscale research letters, 2020, 15: 1-11; https://doi.org/10.1186/s11671-020-3283-5

[2] Nadia Jasim Ghdeeb, AIP Conf. Proc. 2591, 040010-1-040010-6; https://doi.org/10.1063/5.0119597

[3] Imran Din, Muhammad; Rani, Aneela, International journal of analytical chemistry, 2016, 2016.1: 3512145; https://doi.org/10.1155/2016/3512145

[4] Ali MY, Abad WK, Roomy HM, Abd AN. 2023, NanoWorld J 9(3): 89-93; https://doi.org/10.17756/nwj.2023-121

[5] Al-Saidi, Muthana, et al., Biomedicine, 2022, 42.6: 1290-1295; https://doi.org/10.51248/.v42i6.2071

[6] Nadia Jasim Ghdeeb, Int. J. Thin. Film. Sci. Tec. 11, No. 1, 115-121 (2022); https://doi.org/10.18576/ijtfst/110115

[7] Iqbal, Javed, et al., Applied Organometallic Chemistry, 2019, 33.8: e4950; https://doi.org/10.1002/aoc.4950

[8] Sabouri, Zahra, et al., Green Chemistry Letters and Reviews, 2021, 14.2: 404-414; https://doi.org/10.1080/17518253.2021.1923824

[9]. Mezher, Thaer A.; ALI, Abdullah M.; ABD, Ahmed N., International Journal of Nanoscience, 2023, 22.04: 2350035; https://doi.org/10.1142/S0219581X23500357

[10] Hrbe, Zainab Ali; Alzubaidy, Muneer H. Jaduaa; Abd, Ahmed N., NeuroQuantology, 2022, 20.7: 3028.

[11] ALI, Tanveer, et al., Ceramics International, 2022, 48.6: 8331-8340; https://doi.org/10.1016/j.ceramint.2021.12.039

[12] Arkan K. Buraihi, Nisreen Kh. Abdalameer and Nadia Jasim Ghadeeb, International Journal of Nanoscience,Vol. 23, No. 5 (2024) 2450005; https://doi.org/10.1142/S0219581X24500054

[13] Ahamed, N. Nasir, et al., Sustainable Chemistry for the Environment, 2024, 5: 100063; https://doi.org/10.1016/j.scenv.2024.100063

[14] Aseel Abdulkreem Hadi, Ban A. Badr, Rana Osama Mahdi, Khawla S. Khashan, Optik, 2020, 219: 165019; https://doi.org/10.1016/j.ijleo.2020.165019

[15] Rahdar, Abbas; Aliahmad, M.; Azizi, Y. NiO nanoparticles: synthesis and characterization. 2015.

[16] Abad, Wedian K., Abd, Ahmed N., Habubi, Nadir Fadhil, Biomedicine and Engineering, 2023, 15(4): 363−368; https://doi.org/10.26599/NBE.2023.9290032

[17] Moorthy, Prakash; Kavitha, Helen P., ACS omega, 2023, 8.16: 14752-14765; https://doi.org/10.1021/acsomega.3c00792

[18] Nimisha, O.K., Mary, Ap Reena, Ramanarayanan, Rajita, IOP Conference Series: Materials Science and Engineering, IOP Publishing, 2022. p. 012010; https://doi.org/10.1088/1757-899X/1258/1/012010

[19] Ismail, Shaymaa N., et al., AIP Publishing, 2022; https://doi.org/10.1063/5.0094140

[20] Altaee, Maha Fakhry, Yaaqoob, Laith A., Kamona, Zaid K., Iraqi Journal of Science, 2020, 2888-2896; https://doi.org/10.24996/ijs.2020.61.11.12

[21] Abd, Ahmed N, Al-Marjani, Mohammed F., Kadham, Zahraa A., International Journal of Thin Film Science and Technology, Vol. 7. No. 1, January 2018, PP: 43-47, https://doi.org/10.18576/ijtfst/070106